A NEW IMAGING TECHNIQUE BASED ON THE NONLINEAR PROPERTIES OF TISSUES

Michalakis A. Averkiou, David N. Roundhill, and Jeffry E. Powers

ATL Ultrasound, Post Office Box 3003
Bothell, Washington, 98041-3003

ABSTRACT

Finite amplitude sound propagating in a medium undergoes distortion due to the nonlinear properties of the medium. The nonlinear distortion produces harmonic (and subharmonic) energy in the propagating signal. The amplitudes used by commercial medical scanners during routine diagnostic scanning are in most cases finite and thus within the range that produces nonlinear distortion. Thermoviscous absorption of tissue which is frequency dependent rapidly dissipates this harmonic energy. This has led to the widely held assumption that nonlinear distortion was not a significant factor in medical diagnostic imaging. However, the wide dynamic range, digital architecture, and the signal processing capabilities of modern diagnostic ultrasound systems make it possible to utilize this tissue generated harmonic energy for image formation. These images often demonstrate reduced nearfield artifacts and improved tissue structure visualization. Previously, those images were believed to be the result of transmitted second harmonic energy. It is shown that the nonlinear properties of tissue are the major contribution of harmonic images.

INTRODUCTION

Medical ultrasound scanners are widely used in hospitals all over the world for diagnostic purposes. While many technological improvements have been achieved over the years that resulted in better images, a large number of patients are still difficult to image due to problems such as tough windows, inhomogeneous skin layers, and limited penetration.

In the recent years contrast agents have been introduced to enhance ultrasound images. Contrast agents are gas filled microbubbles with typical diameters of a few microns that are injected into the blood and oscillate under insonification and thus enhance the ultrasonic images. The nonlinear nature of bubble dynamics lends itself to harmonic imaging, a procedure by which energy is being transmitted in a fundamental frequency f and an image is formed with energy at the second harmonic $2f$. One of the original assumptions in attempting harmonic imaging was that tissue may be modeled as linear and thus only the contrast microbubbles in the blood would produce second harmonic signals. The harmonic images before contrast microbubble injection were originally believed to be the result of transmitted second harmonic energy from the transducer or incomplete filtering out of the fundamental.

Propagation of sound beams in water is known to be nonlinear, giving rise to waveform distortion, harmonic generation, and eventually shock formation. Water is quite unique in terms of harmonic generation because, while it has a nonlinearity coefficient that is very similar to the vast majority of fluids and more importantly biological tissues, it has an extremely low absorption coefficient (in most cases may be modeled as lossless) and thus the shifting of energy to higher frequency bands (due to distortion) is easily observed. Tissue, on the other hand, has a very similar nonlinearity coefficient to water but a considerably higher absorption coefficient and thus any harmonic generation is accompanied by excessive absorption and is not easily observed.

Some of the characteristics of the nonlinearly generated second harmonic beams are a narrower beam, lower sidelobes than the fundamental,[1] and beam formation in a cumulative process–the second harmonic is drawing energy continually along propagation from the fundamental. These characteristics are contributing to axial resolution improvements, reduction of multiple reflections due to tough windows, and clutter reduction due to inhomogeneities in the tissue and skin layers.

The sound beams used in diagnostic ultrasound systems may be modeled with the Khokhlov-Zabolotskaya-Kuznetsov (KZK) equation.[2, 3] This model accounts for diffraction, absorption and nonlinearity. Since the properties of tissue are readily available in literature, including the coefficient of nonlinearity, nonlinear propagation through tissue can be modeled with the KZK

0-7803-4153-8/97/$10.00

equation. In doing so we can get an estimate of the degree of harmonic generation that takes place in biological tissues. This would be an indicator as to whether there would be enough energy in the second harmonic band to form an image.

In this paper we first discuss the basics of nonlinear beam propagation and present a theoretical model. Experiments of harmonic generation in water and beef tissue using an ATL *HDI-3000* medical scanner are presented next. The implementation of harmonic imaging on the ATL HDI-3000 is discussed. Radio-frequency data of backscattered signals from cardiac and abdominal images are shown to indicate the level of second harmonic signal available for imaging. The method of frequency compounding and its application to second harmonic imaging is discussed. Images are shown that emphasize the benefits of harmonic imaging.

THEORY

The combined effects of diffraction, absorption, and nonlinearity in directive sound beams are modeled by the KZK nonlinear parabolic wave equation:

$$\frac{\partial^2 p}{\partial z \partial t'} = \frac{c_0}{2}\nabla_r^2 p + \frac{\delta}{2c_0^3}\frac{\partial^3 p}{\partial t'^3} + \frac{\beta}{2\rho_0 c_0^3}\frac{\partial^2 p^2}{\partial t'^2}, \qquad (1)$$

where p is the sound pressure, z the coordinate along the axis of the beam, $\nabla_r^2 = \partial^2/\partial r^2 + r^{-1}(\partial/\partial r)$, r is the transverse radial coordinate (the sound beam is assumed to be axisymmetric for simplicity), $t' = t - z/c_0$ the retarded time, and c_0 the sound speed. The first term on the right-hand side of Eq. (1) accounts for diffraction. The second term accounts for thermoviscous dissipation (δ is the diffusivity of sound,[4] which accounts for losses due to shear viscosity, bulk viscosity, and heat conduction) and is proportional to the absorption coefficient α. The third term accounts for quadratic nonlinearity of the fluid (β is the coefficient of nonlinearity,[5] $\beta = 1 + B/2A$, and ρ_0 is the ambient density of the fluid). In general, Eq. (1) is an accurate model of the sound field produced by directive sound sources ($ka \gg 1$, where k characterizes the wavenumber and a the radius of the source) at distances beyond a few source radii and in regions close to the axis of the source, the paraxial region (up to about 20° off the z axis in the farfield). These restrictions are satisfied in most practical applications of directive sound beams, including diagnostic ultrasound. The KZK equation has been used by many researchers and was found to be in excellent agreement with experiments.[6, 7, 8]

Nonlinear waveform distortion in water is easily observed due to its low thermoviscous absorption coefficient. Tissue has similar nonlinear properties with water but it also has a much higher absorption coefficient which results in a faster dissipation of the harmonic energy. This has led researchers to believe that tissue may be modeled as linear. Table 1 shows the coefficient of nonlinearity for various fluids and tissues.[9]

Material	Coeff. of Nonlin., $\beta = 1 + B/2A$
water	3.5
amniotic fluid	3.6
kidney	5.5
liver	4.5
spleen	5.0
muscle	3.9
lymph node	5.1
brain	4.3
fat	6.5

Table 1: Coefficient of nonlinearity (β) for various fluids and tissues.

Equation(1) is used here to model propagation of an imaging ultrasound beam in tissue. The tissue and source parameters are discussed first. The model assumes a circular source and we use a radius of $a = 1$ cm which has roughly the same area as the P3-2 phased array of an ATL HDI-3000. The frequency used is $f = 2$ MHz. For focal length we use $d = 10$ cm. The assumed speed of sound is $c = 1550$ cm/s, the density is $\rho = 1050$ kg/m^3, and the coefficient of nonlinearity is $\beta = 5$, which is higher than water ($\beta_{water} = 3.5$) as is the case for almost all kinds of tissues. For absorption we use 0.3 dB/cm at 1 MHz with a frequency dependence $f^{1.1}$. At $f = 2$ MHz the absorption is $\alpha_0 = 6.4$ dB/cm.

The source pressure very close to the P3-2 phased array was measured with a Marconi membrane hydrophone for various system settings. During those measurements we have observed that the second harmonic level at about 5 mm away from the source is 30 dB down from the fundamental. Since this measurement is taken very close to the source, the edge wave (diffracted) and the center wave (direct) are well separated and no focusing has taken place yet. For a setting where the Mechanical Index (MI) is 1.0 the measured source pressure is about 0.5 MPa. In our modeling here we use $p_0 = 372$ kPa, a value that is even less than measured to emphasize that nonlinear propagation takes place at even lower amplitudes. We used a numerical code that solves Eq.(1) in the frequency domain. The numerical code uses three nondimensional parameters:

- An absorption parameter, $A = \alpha_0 d$
- A nonlinearity parameter, $N = d/l_p$, where $l_p =$

$\rho_0 c^3/\beta\omega p_0$ is the plane wave shock formation distance, and

- The focusing gain, $G = ka^2/2d$

According to the tissue and source parameters listed above the nondimensional parameters were $A = 0.74$, $N = 0.60$, and $G = 4.23$.

In Fig. 1 the numerical results for propagation curves for the first three harmonic components in tissue are shown. The second harmonic component maximum is

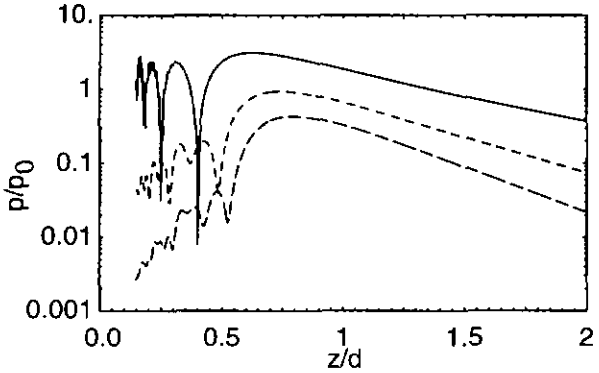

Figure 1: Numerical results for propagation curves for the first three harmonic components in tissue for $A = 0.74$, $N = 0.60$, and $G = 4.23$.

shifted by about 15% away from the transducer. This is expected because the second harmonic component is built from the fundamental in a cumulative process. We may think of it as being created by a virtual source which is a volume beginning in front of the actual source and extending along the propagation path. The extend of this virtual source is limited by thermoviscous losses (attenuation) and in most practical tissue related cases may extend up to the focal region. It is also a more focused beam. Since near the transducer it is still in an early development state it will not interfere with path obstacles that may cause clutter. Here we are reminded that the actual transducers are rectangular (and not circular as the model assumes) and at times source apodization is used. Thus, the structure shown here for a circular source with deep nulls is overemphasized. However, the general trends are still the same.

In Fig. 2 the numerical results for beam patterns at various ranges for the first three harmonic components in tissue are shown. At all ranges it is observed that the second (and third) harmonic beam patterns are narrower than the fundamental as expected. In addition, the sidelobes of the harmonic beams are lower than those of the fundamental. Even though a very

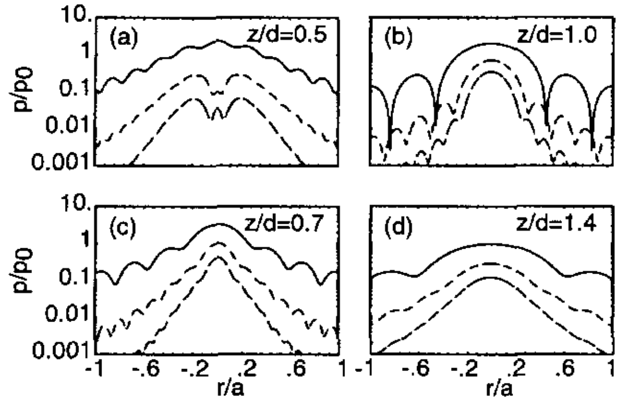

Figure 2: Numerical results for beam patterns for the first three harmonic components in tissue for $A = 0.74$, $N = 0.60$, and $G = 4.23$.

typical tissue absorption is used in the model, there is still a considerable amount of second harmonic energy at the focus where the second harmonic is only 9 dB down. The beam pattern at the focus ($z/d = 1.0$) shows the classic Bessel directivity for the fundamental. We note that the second harmonic beam pattern has extra sidelobes at locations where the fundamental has nulls. These extra sidelobes are often called "fingers" and have been observed in previously published experiments.[10, 11]

EXPERIMENTS

In this section we show measurements of the beam produced by an ATL HDI-3000 P3-2 phased array in water and beef tissue. In these measurements we address the question of whether the second harmonic present is due to nonlinear propagation or direct transmit at twice the fundamental frequency.

In Fig. 3 the measured fundamental and second harmonic beam patterns at the focus in the elevation and transverse direction, respectively, are shown. All measurements presented here were taken with a Marconi membrane hydrophone. The output of the ultrasound system was such that $MI = 0.3$ (this would be the MI reading in tissue) and a 3 cycle tone burst at 2 MHz was used. The second harmonic beam patterns are narrower beams than their corresponding fundamental beam patterns, as expected. In general, an increase in frequency while keeping all other parameters constant results in a narrower beam. However, the second harmonic beam patterns shown in Fig. 3 show better sidelobe suppression. The fundamental sidelobes in the elevation plane are at about 10 dB down from the main lobe and 14 dB in the scanplane, whereas the second

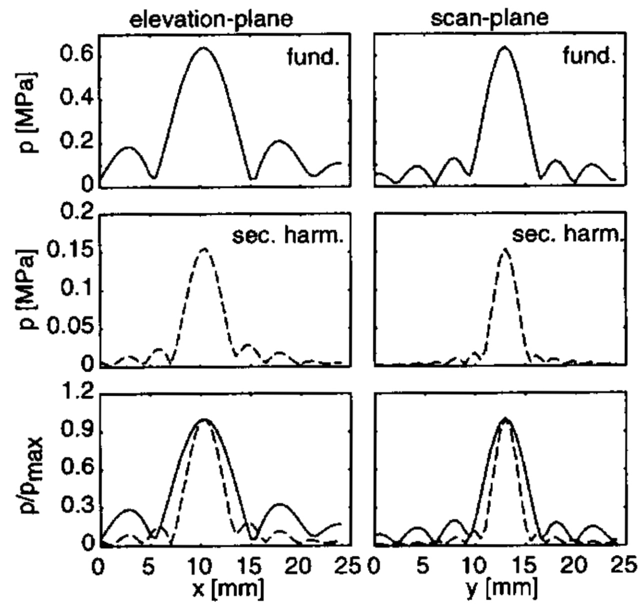

Figure 3: Measurements of focal beam patterns of a P3-2 phased array.

harmonic sidelobes are 16 dB and 20 dB down, respectively.

Extra sidelobes or fingers appear at transverse positions where the fundamental has a null as in Fig. 2. Figure 4 shows beam patterns in dB scale for a slightly higher output setting, $MI = 0.6$. We note the similarity with Fig. 2b. If direct transmit from the transducer

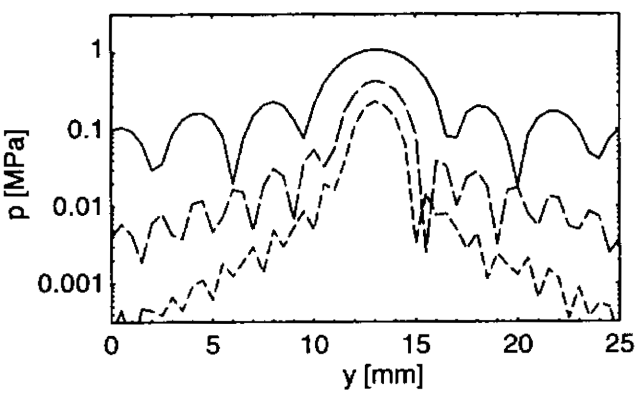

Figure 4: Measurements of focal beam patterns in dB scale of a P3-2 phased array.

at a frequency twice the fundamental was the cause of the second harmonic component, the finger-structure would not be present.

Harmonic generation in beef tissue was also measured. The set-up in Fig. 5 was used. The beef tissue was only 5 mm away from the transducer or the hydrophone. A 3-cycle tone burst was used and the output setting of the ultrasound system was such that $MI = 0.5$. The focus was at 8 cm and the hydrophone was placed at 10 cm.

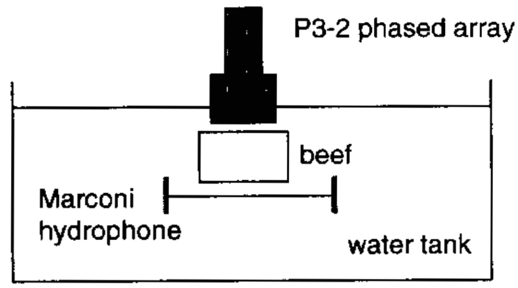

Figure 5: Experimental set-up for measurement of harmonic generation in beef tissue.

Before the beef tissue was placed in the tank we measured the waveform very close to the transducer (5 mm away). As shown in Fig. 6(a) the second harmonic was 30 dB below the fundamental at this range. Next

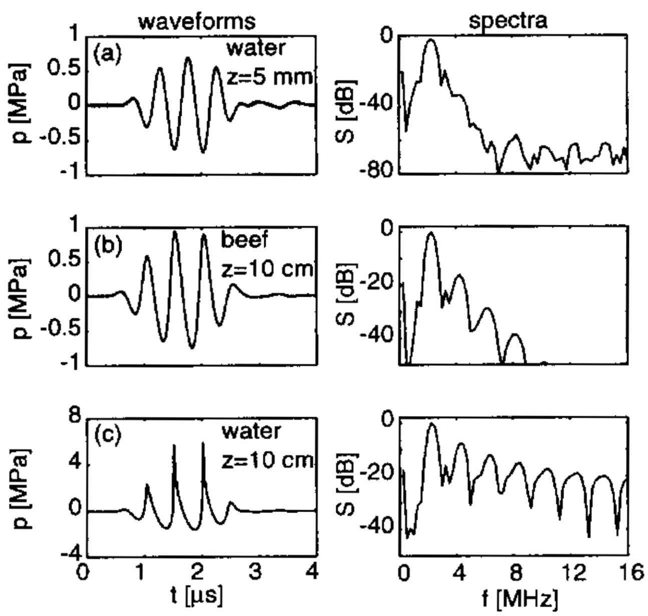

Figure 6: Measured waveforms at the transducer surface (a), and at 10 cm away from the transducer after propagation through beef tissue (b) and water (c).

we measured the waveform at the beef exit plane (10 cm away from the transducer), as shown in Fig. 6(b). Finally, we removed the tissue and we measured the waveform in Fig. 6(c). In the spectrum for the beef waveform we see a strong second harmonic present, and even the 4th harmonic is within 40 dB. Comparing the beef and water spectra we also calculated the attenuation coefficient to be 0.8 dB/cm at 2 MHz, 1.6 dB/cm at 4, and 2.4 dB/cm at 8, or 0.4 dB/cm/MHz.

Beam patterns at the exit plane of tissue were measured next as shown in Fig. 7. Harmonic generation down to three harmonic components is observed for a power setting of $MI = 1.0$ (a setting higher than the one used in Fig. 6). The fourth harmonic component was also measured but it is not shown here. The finger structure, a feature very prominent of nonlinear generation is seen in both the 2nd and 3rd harmonics. The asymmetry in the beam patterns comes from the asymmetry of the sample (not perfectly rectangular) and from the movement in the hydrophone (not perfectly aligned).

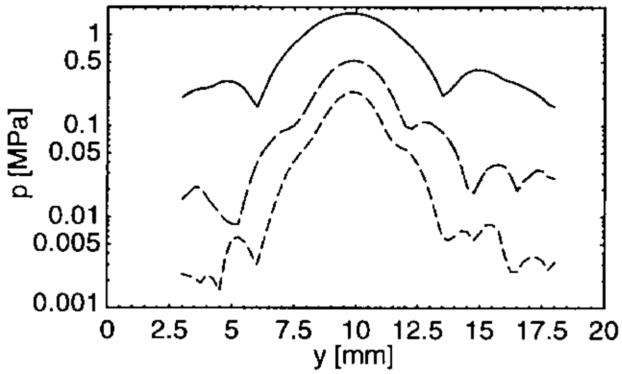

Figure 7: Beam patterns of the first three harmonic components after propagation through beef tissue.

APPLICATION TO MEDICAL IMAGING

The implementation of harmonic imaging on an ATL HDI-3000 is discussed here. For the cardiology application a 4-cycle tone burst at 1.67 MHz is used. This is at a lower frequency than what is used in conventional imaging in order to accommodate both the transmit and receive bands within the band width of the P3-2 phased array. It is also a longer pulse to enable separation of the received fundamental and second harmonic bands. A similar approach is used in radiology. In Fig. 8 we show the spectrum of typical RF-signals that are collected back at the transducer. This is the average spectrum of 30 scanlines (out of 128-line sector) that pass through the myocardium. The total range of this data is 2 cm. For this example the second harmonic level received is 30 dB down from the fundamental. Here we are reminded that the transducer has different sensitivity at the fundamental and second harmonic.

The speckle artifact associated with ultrasound imaging may be reduced by various frequency compounding (or diversity) approaches.[12] These compounding methods involve averaging signals from the same sample region that have partially decorrelated speckle patterns. One approach to achieving decorrelation of speckle is to form detected signals form two or more frequency bands. When these detected signals are averaged, the speckle artifact is reduced.

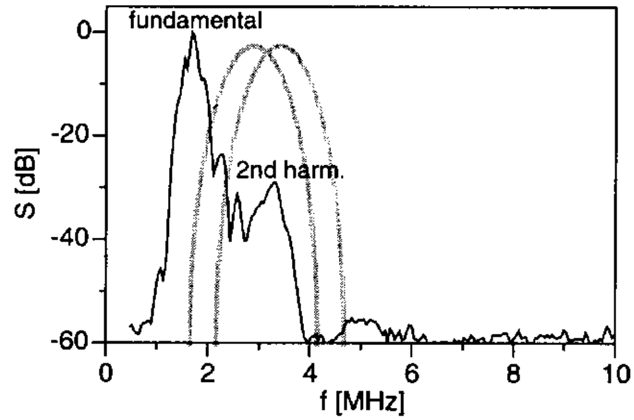

Figure 8: Spectrum of RF-signals from a cardiac image.

Tissue harmonic imaging has been applied for both cardiology and radiology settings. In both cases the improvement of images was in terms of clutter and haze reduction from multipath reflection in the nearfield in patients with tough windows and tough skin layer aberration. The endocardial boarders are delineated better in harmonic mode and the chambers are easier to see. The presence of a fluid path like the left ventricle in cardiology, or the aorta and the gal bladder in radiology, seem to help the enhancement of surrounding borders and supplied better tissue definition.

In Fig. 9 a renal cyst is imaged in conventional (fundamental) mode and in Fig. 10 in harmonic mode. The cyst is better defined in harmonic mode. In addition, the haze present in conventional mode (a problem typically encountered with 30% of the patients in radiology) is removed in the harmonic mode. This observation was made repeatedly with many patients during clinical evaluations of harmonic imaging.

CONCLUSION

A new imaging technique, Tissue Harmonic Imaging, has been presented where the images are formed from the second harmonic energy that results from nonlinear propagation through tissue. A diagnostic ultrasound beam was modeled with the KZK equation and the level of harmonic generation was predicted first. Hydrophone measurements of a diagnostic ultrasound beam in water and in beef tissue were used to prove that

Figure 9: Renal cyst in fundamental mode.

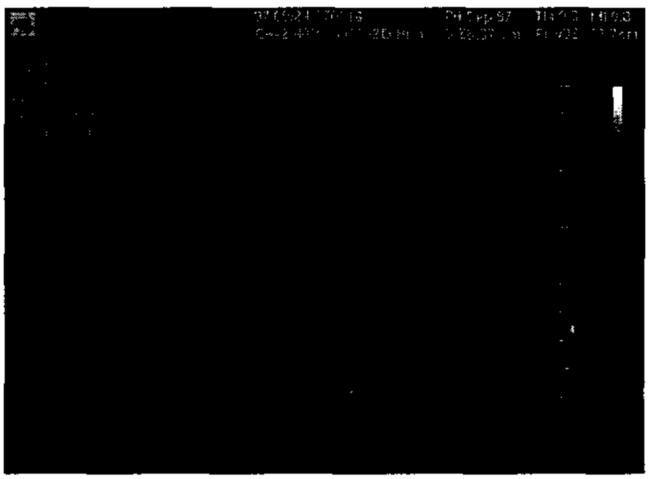

Figure 10: Renal cyst in harmonic mode.

the second harmonic signals that are present and used for imaging are due to nonlinear propagation and not due to direct transmit of the harmonic frequency. The extra sidelobes shown in the literature in the past as an indicator of harmonic generation were also measured in the field of a diagnostic beam. The harmonic beams generated are narrower than the fundamental beams that are originally transmitted, have lower sidelobes, and suffer less aberration. The images that are formed with this technique offer better border definition, give better tissue contrast, and show clear improvements in cases where tough windows and highly inhomogeneous paths are encountered.

References

[1] T. Christopher, "Finite amplitude distortion-based inhomogeneous pulse echo ultrasonic imaging," *IEEE Trans. Ultrason. Ferr. Freq. Control* **44**, 125–130 (1997).

[2] E. A. Zabolotskaya and R. V. Khokhlov, "Quasi-plane waves in the nonlinear acoustics of confined beams," *Sov. Phys. Acoust.* **15**, 35–40 (1969).

[3] V. P. Kuznetsov, "Equation of nonlinear acoustics," *Sov. Phys. Acoust.* **16**, 467–470 (1970).

[4] J. Lighthill, *Waves in Fluids* (Cambridge University Press, Cambridge, 1980), pp. 78–83.

[5] R. T. Beyer, "Parameter of nonlinearity in fluids," *J. Acoust. Soc. Am.* **32**, 719–721 (1960).

[6] M. A. Averkiou and M. F. Hamilton, "Nonlinear distortion of short pulses radiated by plane and focused circular pistons," *J. Acoust. Soc. Am.* **102**,(1997).

[7] A. C. Baker and V. F. Humphrey, "Nonlinear propagation of short ultrasonic pulses in focused fields," in *Frontiers of Nonlinear Acoustics: Proceedings of 12th ISNA*, edited by M. F. Hamilton and D. T. Blackstock (Elsevier Applied Science, London, 1990), pp. 185–190.

[8] A. C. Baker, A. M. Berg and J. N. Tjøtta, "The nonlinear pressure field of plane,rectangular apertures: Experimental and theoretical results," *J. Acoust. Soc. Am.* **97**, pp. 3510–3517 (1997).

[9] Francis A. Duck, *Physical properties of tissue: a comprehensive reference book* (Academic Press, London, San Diego, 1990), p. 98.

[10] M. A. Averkiou and M. F. Hamilton, "Measurements of harmonic generation in a focused finite-amplitude sound beam," *J. Acoust. Soc. Am.* **98**, 3439–3442 (1995).

[11] J. A. TenCate, "An experimental investigation of the nonlinear pressure field produced by a plane circular piston," *J. Acoust. Soc. Am.* **94**, 1084–1089 (1993).

[12] Frederic L. Lizzi, Marek Elbaum, Ernest Feleppa, "*Frequency diversity for image enhancement*," United States Patent 4,561,019, Dec. 1985